A Theoretical Study of the Dynamic Behavior of Alkane Hydroxylation by a Compound I Model of Cytochrome P450

Kazunari Yoshizawa,* Takashi Kamachi,† and Yoshihito Shiota

Contribution from the Institute for Fundamental Research of Organic Chemistry, Kyushu University, Fukuoka 812-8581, Japan

Received March 5, 2001. Revised Manuscript Received May 22, 2001

Abstract: Dynamic aspects of alkane hydroxylation mediated by Compound I of cytochrome P450 are discussed from classical trajectory calculations at the B3LYP level of density functional theory. The nuclei of the reacting system are propagated from a transition state to a reactant or product direction according to classical dynamics on a Born−Oppenheimer potential energy surface. Geometric and energetic changes in both low-spin doublet and high-spin quartet states are followed along the ethane to ethanol reaction pathway, which is partitioned into two chemical steps: the first is the H-atom abstraction from ethane by the iron−oxo species of Compound I and the second is the rebound step in which the resultant iron−hydroxo complex and the ethyl radical intermediate react to form the ethanol complex. Molecular vibrations of the C−H bond being dissociated and the O−H bond being formed are significantly activated before and after the transition state, respectively, in the H-atom abstraction. The principal reaction coordinate that can represent the first chemical step is the C−H distance or the O−H distance while other geometric parameters remain almost unchanged. The rebound process begins with the iron−hydroxo complex and the ethyl radical intermediate and ends with the formation of the ethanol complex, the essential process in this reaction being the formation of the C−O bond. The H−O−Fe−C dihedral angle corresponds to the principal reaction coordinate for the rebound step. When sufficient kinetic energy is supplied to this rotational mode, the rebound process should efficiently take place. Trajectory calculations suggest that about 200 fs is required for the rebound process under specific initial conditions, in which a small amount of kinetic energy (0.1 kcal/mol) is supplied to the transition state exactly along the reaction coordinate. An important issue about which normal mode of vibration is activated during the hydroxylation reaction is investigated in detail from trajectory calculations. A large part of the kinetic energy is distributed to the C−H and O−H stretching modes before and after the transition state for the H-atom abstraction, respectively, and a small part of the kinetic energy is distributed to the Fe−O and Fe−S stretching modes and some characteristic modes of the porphyrin ring. The porphyrin marker modes of ν_3 and ν_4 that explicitly involve Fe−N stretching motion are effectively enhanced in the hydroxylation reaction. These vibrational modes of the porphyrin ring can play an important role in the energy transfer during the enzymatic process.

Introduction

Cytochrome P450 enzymes catalyze the addition of molecular oxygen to nonactivated hydrocarbons under physiological conditions.[1,2] The mechanism by which cytochrome P450 is able to carry out the remarkably difficult hydroxylation of C−H bonds in alkanes and other compounds has been a central issue to be elucidated in biological inorganic chemistry. The active electrophilic oxidant in P450 usually has been assumed to be an oxo-ferryl ($O{=}Fe^{IV}$) porphyrin π-cation radical. A consensus view of the hydroxylation mechanism evolved over the past two decades, primarily based on two mechanistic parameters, stereochemistry and kinetic isotope effects. Observed large kinetic isotope effects ($k_H/k_D > 10$)[3,4] and loss of stereochemistry[4−6] in P450-catalyzed hydroxylation reactions prefer a nonconcerted mechanism to a concerted "oxene" insertion mechanism, which was proposed in an earlier study.[7] In the nonconcerted mechanism, the iron−oxo species abstracts an H atom from substrate to give an iron−hydroxo species and an alkyl radical intermediate, followed by rapid transfer of the iron-bound hydroxyl radical to the alkyl radical. Thus, this so-called oxygen rebound mechanism consists of abstraction and recombination processes. Strong support for this mechanism has come from the functional P450 model systems developed by Groves and co-workers.[8,9]

This mechanistic picture became questionable when ultrafast "radical clock" substrates that have highly strained cyclic structures were used to measure the time for the oxygen rebound step. Newcomb, Hollenberg, and their co-workers found that

* To whom correspondence should be addressed. E-mail: kazunari@ms.ifoc.kyushu-u.ac.jp.

† Graduate student from the Department of Molecular Engineering, Kyoto University.

(1) *Cytochrome P450: Structure, Mechanism, and Biochemistry*, 2nd ed.; Ortiz de Montellano, P. R., Ed.; Plenum: New York, 1995.

(2) Sono, M.; Roach, M. P.; Coulter, E. D.; Dawson, J. H. *Chem. Rev.* **1996**, *96*, 2841.

(3) Hjelmeland, L. M.; Aronow, L.; Trudell, J. R. *Biochem. Biophys. Res. Commun.* **1977**, *76*, 541.

(4) Groves, J. T.; McClusky, G. A.; White, R. E.; Coon, M. J. *Biochem. Biophys. Res. Commun.* **1978**, *81*, 154.

(5) Gelb, M. H.; Heimbrook, D. C.; Mälkönen, P.; Sligar, S. G. *Biochemistry* **1982**, *21*, 370.

(6) White, R. E.; Miller, J. P.; Favreau, L. V.; Bhattacharyaa, A. *J. Am. Chem. Soc.* **1986**, *108*, 6024.

(7) Daly, J. *Handb. Exp. Pharmacol.* **1971**, *28*, 285.

(8) Groves, J. T.; Haushalter, R. C.; Nakamura, M.; Nemo, T. E.; Evans, B. J. *J. Am. Chem. Soc.* **1981**, *103*, 2884.

(9) Groves, J. T. *J. Chem. Educ.* **1985**, *62*, 928.

10.1021/ja010593t CCC: $20.00
Published on Web 09/12/2001

measured radical lifetimes are too short ($\tau = 80-200$ fs) to correspond to a real free radical intermediate[10−12] and have no correlation with independently clocked rearrangement lifetimes of the free radicals. They suggested using a ultrafast radical clock substrate that can distinguish between radical and carbocation intermediates that production of cationic intermediates is a common feature of P450-catalyzed hydroxylation reactions. They proposed that these species are most likely protonated alcohols produced by insertion of OH^+ in reactions of the iron−hydroperoxo species formed in the natural course of P450 oxidation reactions. Coon et al. recently proposed that epoxidation and hydroxylation reactions can be mediated by both iron−hydroperoxo and iron−oxo species.[13,14] Thus, the mechanistic picture of the hydroxylation reaction is more complicated than previously thought.

Quantum chemical calculations at various levels of theory[15−18] have shed new light on the structures and the catalytic functions of Compound I intermediates of oxidative heme enzymes. With density functional theory (DFT), Harris and Loew investigated the proton-assisted pathway to formation of cytochrome P450 Compound I,[19] and Siegbahn et al. studied the mechanisms of O−O bond breaking and Compound I formation in heme peroxidases.[20] Shaik and collaborators investigated some important mechanistic aspects of P450-catalyzed hydroxylation reactions and indicated the participation of "two-state reactivity" in the C−H bond dissociation process and in the resultant iron−hydroxo intermediate.[21−23] They recently found, using a Compound I model with SH^- as the proximal ligand, that the transition state for the rebound step lies 5 kcal/mol above the iron−hydroxo species on the high-spin quartet potential energy surface whereas there is no such transition state on the low-spin doublet one.[24,25] According to their proposal, the doublet pathway cannot endow a radical intermediate with a significant lifetime because it is barrier-free or very flat. In contrast, an alkyl radical will be produced on the quartet pathway and will face a rebound barrier, which can lead to a finite lifetime of the radical intermediate.

Compound I is widely believed from experimental and theoretical investigations to be best formulated as an oxo−ferryl ($O{=}Fe^{IV}$) porphyrin π-cation radical species.[1,2] This picture was reconsidered from experimental and theoretical investigations particularly in thiolate-ligated heme enzymes. From experimental aspects, Meunier and co-workers proposed the existence of a sulfur radical species as a route to reduce the $O{=}Fe^{V}$ to $O{=}Fe^{IV}$ species in the stabilized form of Compound I of P450.[26,27] Trautwein et al. discussed in detail different electronic states of Compound I with the radical located in the a_{1u} or a_{2u} π orbital of the porphyrin ring or in the lone-pair orbital of the proximal ligand (chlorine, imidazole, and CH_3S^-).[28,29] Green indicated that the electronic structure of Compound I depended dramatically upon the nature of the proximal ligand and suggested that an alternative formulation of Compound I with sulfur radical may be more appropriate rather than that with porphyrin π-cation radical.[30−32] We suggested from the ionization potentials of HS^-, CH_3S^-, $CysS^-$, and imidazole that the thiolate ligands may release one electron to form a sulfur radical species while the imidazole ligand is unlikely to be oxidized.[33] Recently, Shaik et al. indicated that hydrogen bonding and medium polarization effects should cause a dramatic shift of the spin density, which is localized more heavily on the porphyrin ring than the axial thiolate ligand.[34]

The kinetic isotope effect (k_H/k_D) is an important measure in discussing how H-atom abstraction from substrate takes place in catalysts and enzymes. The oxygen rebound mechanism is supported by observed large kinetic isotope effects as well as considerable loss of stereochemistry at a carbon atom of the substrate.[1,2] Jones et al. recently found that the k_H/k_D values of P450-mediated H-atom abstraction from several substrates are nicely correlated with those of H-atom abstraction by the *tert*-butoxyl radical, providing evidence for a common H-atom abstraction mechanism, but that the k_H/k_D values are rather small, 2−6.[35] We calculated the k_H/k_D values for the H(D) atom abstraction using C_2H_6, CH_2DCH_3, CD_3CH_3, and C_2D_6 as substrates, demonstrating that not only the C−H(D) bond being cleaved but also other molecular moieties play an important role in determining the kinetic isotope effect.[36] The kinetic isotope effect is also more complicated than previously thought.

In previous work,[37] we carried out trajectory calculations on the methane to methanol conversion mediated by the bare FeO^+ complex to increase our knowledge of the dynamic aspect of alkane hydroxylation, demonstrating that both the H-atom abstraction and the methyl migration, which corresponds to the oxygen rebound step, should occur in a time scale of about 100 fs in a concerted manner. We compared the concerted mechanism via a four-centered transition state $\overline{C\cdots H\cdots O-Fe}$ and the radical mechanism via a linear transition state C···H···O−Fe with respect to the rate-determining H-atom abstraction process. We decided to run molecular dynamics simulations on alkane hydroxylation mediated by P450 to derive the dynamic aspects of this important enzymatic reaction. In this article, we discuss

(10) Newcomb, M.; Le Tadic-Biadatti, M.-H.; Chestney, D. L.; Roberts, E. S.; Hollenberg, P. F. *J. Am. Chem. Soc.* **1995**, *117*, 12085.
(11) Toy, P. H.; Dhanabalasingam, B.; Newcomb, M.; Hanna, I. H.; Hollenberg, P. F. *J. Org. Chem.* **1997**, *62*, 9114.
(12) Toy, P. H.; Newcomb, M.; Hollenberg, P. F. *J. Am. Chem. Soc.* **1998**, *120*, 7719.
(13) Vaz, A. D. N.; McGinnity, D. F.; Coon, M. J. *Proc. Natl. Acad. Sci. U.S.A.* **1998**, *95*, 3555.
(14) Newcomb, M.; Shen, R.; Choi, S.-Y.; Toy, P. H.; Hollenberg, P. F.; Vaz, A. D. N.; Coon, M. J. *J. Am. Chem. Soc.* **2000**, *122*, 2677.
(15) Strich, A.; Veillard, A. *Nouv. J. Chim.* **1983**, *7*, 347.
(16) Yamamoto, S.; Kashiwagi, H. *Chem. Phys. Lett.* **1988**, *145*, 111.
(17) Ghosh, A.; Almlöf, J.; Que, L., Jr. *J. Phys. Chem.* **1994**, *98*, 5576.
(18) Kuramochi, H.; Noodleman, L.; Case, D. A. *J. Am. Chem. Soc.* **1997**, *119*, 11442.
(19) Harris, D. L.; Loew, G. H. *J. Am. Chem. Soc.* **1998**, *120*, 8941.
(20) Wirstam, M.; Blomberg, M. R. A.; Siegbahn, P. E. M. *J. Am. Chem. Soc.* **1999**, *121*, 10178.
(21) Shaik, S.; Filatov, M.; Schröder, D.; Schwarz, H. *Chem. Eur. J.* **1998**, *4*, 193.
(22) Filatov, M.; Harris, N.; Shaik, S. *J. Chem. Soc., Perkin Trans. 2* **1999**, 399.
(23) Filatov, M.; Harris, N.; Shaik, S. *Angew. Chem., Int. Ed. Engl.* **1999**, *38*, 3510.
(24) Ogliaro, F.; Harris, N.; Cohen, S.; Filatov, M.; de Visser, S. P.; Shaik, S. *J. Am. Chem. Soc.* **2000**, *122*, 8977.
(25) Harris, N.; Cohen, S.; Filatov, M.; Ogliaro, F.; Shaik, S. *Angew. Chem., Int. Ed. Engl.* **2000**, *39*, 2003.
(26) Bernadou, J.; Fabiano, A.-S.; Robert, A.; Meunier, B. *J. Am. Chem. Soc.* **1994**, *116*, 9375.
(27) Bernadou, J.; Meunier, B. *Chem. Commun.* **1998**, 2167.
(28) Zakharieva, O.; Grodzicki, M.; Trautwein, A. X.; Veeger, C.; Rietjens, I. M. C. M. *J. Biol. Inorg. Chem.* **1996**, *1*, 192.
(29) Antony, J.; Grodzicki, M.; Trautwein, A. X. *J. Phys. Chem. A* **1997**, *101*, 2692.
(30) Green, M. T. *J. Am. Chem. Soc.* **1998**, *120*, 10772.
(31) Green, M. T. *J. Am. Chem. Soc.* **1999**, *121*, 7939.
(32) Green, M. T. *J. Am. Chem. Soc.* **2000**, *122*, 9495.
(33) Ohta, T.; Matsuura, K.; Yoshizawa, K.; Morishima, I. *J. Inorg. Biochem.* **2000**, *82*, 141.
(34) Ogliaro, F.; Cohen, S.; de Visser, S. P.; Shaik, S. *J. Am. Chem. Soc.* **2000**, *122*, 12892.
(35) Manchester, J. I.; Dinnocenzo, J. P.; Higgins, L.-A.; Jones, J. P. *J. Am. Chem. Soc.* **1997**, *119*, 5069.
(36) Yoshizawa, K.; Kagawa, Y.; Shiota, Y. *J. Phys. Chem. B* **2000**, *104*, 12365.
(37) Yoshizawa, K.; Shiota, Y.; Kagawa, Y.; Yamabe, T. *J. Phys. Chem. A* **2000**, *104*, 2552.

from trajectory calculations based on density functional theory (DFT) the ethane to ethanol conversion mediated by a Compound I model, with an emphasis on the elucidation of its mechanistic aspects. The present work may be useful for a deeper understanding of the recent radical clock studies on alkane hydroxylation mediated by cytochrome P450.

Model System and Method of Calculation

Although both iron−oxo and iron−hydroperoxo species have been recently proposed as oxidants in cytochrome P450 systems,[13,14] we assumed a porphyrin iron−oxo species as the final oxidant in our theoretical study. Recently, the structure of the ferrous dioxygen adduct of P450cam was determined with 0.91 Å wavelength X-rays; irradiation with a 1.5 Å X-ray resulted in breakdown of the dioxygen molecule to an intermediate that would be consistent with an oxo−ferryl species.[38] Accordingly we used a six-coordinate oxo−ferryl species $Fe^{4+}O^{2-}(C_{20}N_4H_{12})^{-1}(SCH_3)^{-1}$ as Compound I model and ethane as substrate. Thus, the total charge of the model reacting system is neutral. In a previous study, the ionization potentials of various thiolate ligands and imidazole were calculated to better understand the mechanism of the two-electron oxidation process for the formation of Compound I; the order of ionization potential was imidazole $\gg HS^-$ > $CysS^- \sim CH_3S^-$.[39] Therefore CH_3S^- is appropriate as the proximal ligand from the point of view of ionization potential. We considered the low-spin doublet and the high-spin quartet states in analyzing the reaction profile.

We used the spin-unrestricted version of the B3LYP method,[40−43] a hybrid Hartree−Fock/density-functional-theory (DFT) method. This hybrid method consists of the Slater exchange, the Hartree−Fock exchange, the exchange functional of Becke,[40,41] the correlation functional of Lee, Yang, and Parr (LYP),[43] and the correlation functional of Vosko, Wilk, and Nusair.[44] It has been successfully applied to many chemical reactions mediated by transition-metal complexes.[45] Because of the very heavy computational task for trajectory calculations, we used the 3-21G basis set[46−48] for H, C, N, O, S, and Fe and added polarization functions[49] to S although the 3-21G basis set is rather small in the age of computational quantum chemistry. Optimized structures with the 3-21G basis set were in quantitative agreement with those obtained from higher level calculations[36] with a combination of the triple-ζ valence and the D95 basis sets. Harmonic vibrational frequencies were systematically computed to confirm that an optimized geometry correctly corresponds to a local minimum that has only real frequencies or a saddle point that has only one imaginary frequency. The Gaussian 98 program[50] was used for the DFT computations.

Newton's equations of motion were numerically solved to determine positions, velocities, and accelerations for each atom. We used the velocity Verlet algorithm[51,52] for propagating the nuclei classically. We took a time interval of 0.5 fs, which is short enough compared to 12 fs for the period of C−H stretching vibration. The forces were calculated with the B3LYP DFT method according to eq 1, where E^n is the

$$f_i^n = -\nabla_i E^n \tag{1}$$

potential energy of the reacting system in the nth step. The trajectory calculations on the ethane hydroxylation pathway were carried out by solving the equations of motion; thus, in every time step, the wave function was fully converged to the Born−Oppenheimer surface and the first derivatives of the potential energy were calculated. This computational work is very heavy at present.

To start a trajectory calculation, a small amount of kinetic energy (0.1 kcal/mol) was supplied to a transition state moving toward reactant or product along the imaginary mode of vibration. Thus, the reacting system has excess kinetic energy in both reactant and product, whereas it has almost no kinetic energy in the vicinity of the transition state. We then analyzed how the kinetic energy of the reacting system is distributed into vibrational modes along the reaction pathway. Changes in the amplitudes of normal coordinates along the reaction pathway were calculated. The time-dependent equation for the normal coordinates[53] in the trajectory analysis can be written as:

$$Q_i(t) = \sum_{k}^{3N} \sum_{n=-10}^{10} (|X_k(t_{n+1}) - X_k(t_n)|) \sqrt{m_k} L_{ki} \qquad (t_n = t + 0.5n) \tag{2}$$

in which Q_i is the ith normal coordinate, X_k is the kth Cartesian coordinate, m_k is the atomic mass corresponding to X_k, L_{ki} is the kth component of the ith normal mode of the equilibrium geometry, and N is the number of atoms in the system.

Results and Discussion

This section on the results of ethane hydroxylation by a Compound I model is divided into four subsections. We look at computed structures of the reaction species and their energetics to characterize the electronic features of this model enzymatic reaction in the first subsection. The first half of the reaction is the H-atom abstraction from ethane leading to an iron−hydroxo intermediate and ethyl radical. The second half is the rebound step; the resultant iron−hydroxo intermediate and ethyl radical come into contact to form the product complex that involves ethanol as a ligand. In the second and third subsections, we present trajectory calculation results on the H-atom abstraction process and the rebound process, respectively. Finally, we turn our attention to how the kinetic energy of the reacting system is distributed into normal modes of vibration during the model enzymatic reaction.

Energetics for the Reaction Pathway. Before considering trajectory calculations, let us look at the energy profiles along the reaction pathway. Figure 1 demonstrates computed energy diagrams and optimized geometries of various reaction species for the hydroxylation of ethane by a Compound I model of P450 at the B3LYP/3-21G level of theory. The general profiles of the energies and the geometries are very similar to those

(38) Schlichting, I.; Berendzen, J.; Chu, K.; Stock, A. M.; Maves, S. A.; Benson, D. E.; Sweet, R. M.; Ringe, D.; Petsko, G. A.; Sligar, S. G. *Science* **2000**, *287*, 1615.
(39) Matsuura, K.; Shiota, Y.; Ohta, T.; Morishima, I.; Yoshizawa, K. To be submitted for publication.
(40) Becke, A. D. *Phys. Rev. A* **1988**, *38*, 3098.
(41) Becke, A. D. *J. Chem. Phys.* **1993**, *98*, 5648.
(42) Stephens, P. J.; Devlin, F. J.; Chabalowski, C. F.; Frisch, M. J. *J. Phys. Chem.* **1994**, *98*, 11623.
(43) Lee, C.; Yang, W.; Parr, R. G. *Phys. Rev. B* **1988**, *37*, 785.
(44) Vosko, S. H.; Wilk, L.; Nusair, M. *Can. J. Phys.* **1980**, *58*, 1200.
(45) (a) Baker, J.; Muir, M.; Andzelm, J.; Scheiner A. In *Chemical Applications of Density-Functional Theory*; Laird, B. B., Ross, R. B., Ziegler, T., Eds.; ACS Symp. Ser. No. 629; American Chemical Society: Washington, DC, 1996. (b) Koch, W.; Holthausen, M. C. *A Chemist's Guide to Density Functional Theory*; Wiley-VCH: Weinheim, Germany, 2000.
(46) Binkley, J. S.; Pople, J. A.; Hehre, W. J. *J. Am. Chem. Soc.* **1980**, *102*, 939.
(47) Gordon, M. S.; Binkley, J. S.; Pople, J. A.; Pietro, W. J.; Hehre, W. J. *J. Am. Chem. Soc.* **1982**, *104*, 2797.
(48) Dobbs, K. D.; Hehre, W. J. *J. Comput. Chem.* **1987**, *8*, 861.
(49) Pietro, W. J.; Francl, M. M.; Hehre, W. J.; Defrees, D. J.; Pople, J. A.; Binkley, J. S. *J. Am. Chem. Soc.* **1982**, *104*, 5039.
(50) Frisch, M. J.; Trucks, G. W.; Schlegel, H. B.; Scuseria, G. E.; Robb, M. A.; Cheeseman, J. R.; Zakrzewski, V. G.; Montgomery, J. A.; Stratmann, R. E.; Burant, J. C.; Dapprich, S.; Millam, J. M.; Daniels, A. D.; Kudin, K. N.; Strain, M. C.; Farkas, O.; Tomasi, J.; Barone, V.; Cossi, M.; Cammi, R.; Mennucci, B.; Pomelli, C.; Adamo, C.; Clifford, S.; Ochterski, J.; Petersson, G. A.; Ayala, P. Y.; Cui, Q.; Morokuma, K.; Malick, D. K.; Rabuck, A. D.; Raghavachari, K.; Foresman, J. B.; Cioslowski, J.; Ortiz, J. V.; Stefanov, B. B.; Liu, G.; Liashenko, A.; Piskorz, P.; Komaromi, I.; Gomperts, R.; Martin, R. L.; Fox, D. J.; Keith, T.; Al-Laham, M. A.; Peng, C. Y.; Nanayakkara, A.; Gonzalez, C.; Challacombe, M.; Gill, P. M. W.; Johnson, B. G.; Chen, W.; Wong, M. W.; Andres, J. L.; Head-Gordon, M.; Replogle, E. S.; Pople, J. A. *Gaussian 98*; Gaussian Inc.: Pittsburgh, PA, 1998.
(51) Verlet, L. *Phys. Rev.* **1967**, *159*, 98.
(52) Swope, W. C.; Andersen, H. C.; Berens, P. H.; Wilson, K. R. *J. Chem. Phys.* **1982**, *76*, 637.
(53) Taketsugu, T.; Gordon, M. S. *J. Phys. Chem.* **1995**, *99*, 8462.

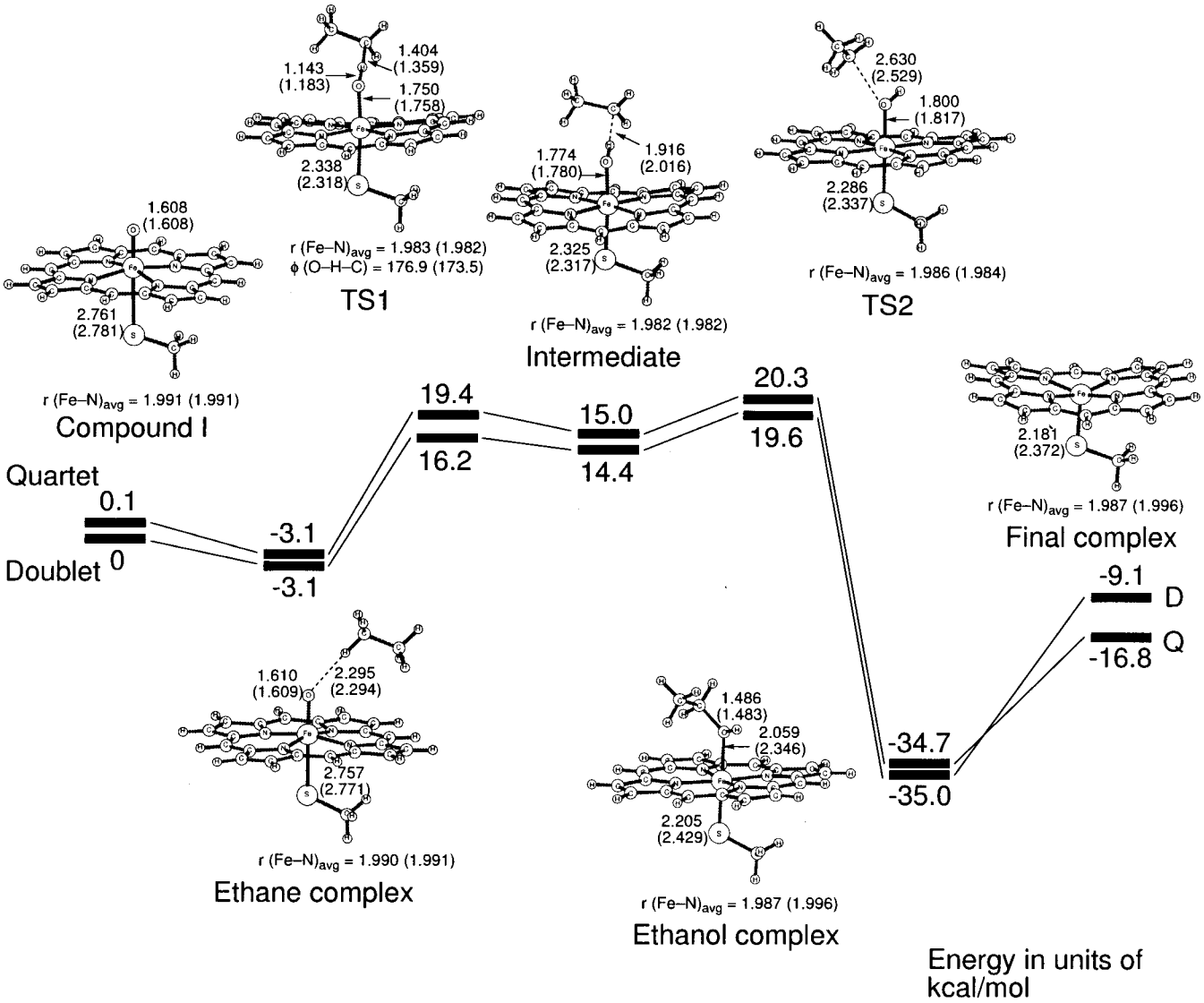

Figure 1. Energy diagrams with optimized structures of the reaction species for the hydroxylation of ethane by a Compound I model in the spin doublet and quartet states. Energy in units of kcal/mol and bond distance in units of Å. The values in parentheses are for the quartet state.

obtained in our previous study with a higher level of theory (B3LYP/TZV+D95).[36] The doublet and quartet potential energy surfaces are close in the entire reaction pathway; for example, the doublet state lies 3.2 kcal/mol below the quartet state in the transition state for the H-atom abstraction (TS1). The optimized structure of TS1 has an imaginary frequency mode; the values in the doublet and quartet states are 834 and 1360 cm^{-1}, respectively. When we follow the low-lying doublet potential energy surface, the C−H bond dissociation should require 19.3 kcal/mol. This value is rather high for an enzymatic reaction, but it is in good agreement with the value for the H-atom abstraction from methane by the bare FeO^+ complex.[54−57] Ethane as well as methane is less reactive than either benzylic or more substituted aliphatic substrates and would require higher activation energy than the substrates that P450 systems are able to hydroxylate. The resultant complex that binds the "ethyl radical" can exist as an intermediate on the potential energy surface, as indicated in the energy diagram.

The second half of the hydroxylation reaction is the so-called rebound step. In both spin states, we found the transition state for the rebound step that connects the intermediate complex and the product complex. The optimized structure of TS2 has an imaginary frequency mode that corresponds to the vibrational mode with respect to the C−O stretching as well as the H−O−Fe−C dihedral angle; the values in the doublet and quartet states are 187 and 196 cm^{-1}, respectively. This chemical step is commonly assumed in the oxygen rebound mechanism. This result is in contrast to the recent finding that a radical intermediate with a finite lifetime will be produced only in the quartet pathway.[24] The barrier height for the rebound process is about 5 kcal/mol measured from the iron−hydroxo complex, and in view of the general profile of the energetics, the reaction intermediate is energetically a very unstable intermediate in both spin states. Its lifetime is expected to be very short. Our results may be consistent with the model involving a radical intermediate in this respect. The product complex that has ethanol as a ligand is very stable in energy. We consider that both doublet and quartet spin states should be responsible for the hydroxylation reaction with respect to the H-atom abstraction and the rebound steps. This is one of the most important aspects in alkane hydroxylation mediated by cytochrome P450 as well as

(54) Yoshizawa, K.; Shiota, Y.; Yamabe, T. *Chem. Eur. J.* **1997**, *3*, 1160.
(55) Yoshizawa, K.; Shiota, Y.; Yamabe, T. *J. Am. Chem. Soc.* **1998**, *120*, 564.
(56) Yoshizawa, K.; Shiota, Y.; Yamabe, T. *Organometallics* **1998**, *17*, 2825.
(57) Shiota, Y.; Yoshizawa, K. *J. Am. Chem. Soc.* **2000**, *122*, 12317.

Table 1. Calculated Mulliken Charges and Spin Densities for the Fe and O Atoms and the CH_3S and Porphyrin (Por) Moieties with Spin Densities in Parentheses

	Fe	O	CH_3S	Por
		doublet state		
Compound I	1.3 (1.4)	−0.4 (0.6)	0.0 (−0.8)	−0.9 (−0.2)
ethane complex	1.3 (1.5)	−0.4 (0.6)	0.0 (−0.9)	−0.9 (−0.2)
TS1	1.3 (1.9)	−0.1 (−0.1)	−0.2 (−0.1)	−1.0 (−0.1)
intermediate	1.3 (2.0)	−0.2 (0.1)	−0.2 (0.0)	−0.9 (−0.1)
TS2	1.3 (1.8)	−0.2 (0.2)	−0.2 (0.0)	−0.9 (−0.2)
ethanol complex	1.3 (1.1)	−0.1 (0.0)	−0.3 (0.0)	−1.2 (−0.1)
final complex	1.3 (1.1)		−0.3 (−0.1)	−1.0 (0.0)
		quartet state		
Compound I	1.3 (1.4)	−0.4 (0.6)	0.0 (0.8)	−0.9 (0.2)
ethane complex	1.3 (1.4)	−0.4 (0.6)	−1.0 (0.8)	−0.8 (0.2)
TS1	1.3 (1.7)	−0.1 (0.6)	−0.2 (−0.2)	−0.9 (0.3)
intermediate	1.3 (1.9)	−0.2 (0.2)	−0.2 (0.0)	−0.9 (−0.1)
TS2	1.3 (2.1)	−0.2 (0.1)	−0.2 (0.1)	−0.9 (−0.1)
ethanol complex	1.2 (2.7)	−0.1 (0.0)	−0.4 (0.3)	−1.0 (0.0)
final complex	1.3 (2.7)		−0.4 (0.3)	−0.9 (0.0)

by other iron−oxo complexes. This electronic feature is consistent with the two-state reactivity paradigm proposed by Shaik et al.[58−60]

Computed atomic charges and spin densities for the reaction species are listed in Table 1. The Compound I model possesses three unpaired electrons, two of which are localized parallelly in the FeO group while the third electron, which determines its spin state, is distributed on the thiolate ligand as well as on the porphyrin ring. Calculated spin densities on the porphyrin ring and the CH_3S group are 0.2 and 0.8, respectively; thus, this model can be viewed as a sulfur radical species. As mentioned above, hydrogen bonding and polarization effects will change Compound I from a thiolate radical species to a porphyrin cation radical species.[34] It is therefore interesting to look in detail at how such environmental factors change the reactivity of Compound I. However, we consider in first approximation that the reactivity is not significantly changed because the change in the spin density on the oxygen atom that dominates the reactivity of metal−oxo species is small under different environmental conditions.

Let us look at the reaction intermediate. Calculated total charge (and the total spin density) on the generated "ethyl radical" is 0.0 (−1.0) and +0.1 (+1.0) in the doublet and quartet states, respectively, and therefore the C−H bond is homolytically cleaved and mechanisms involving carbocations and carbanions may be ruled out. The binding energy for the intermediate complex is about 2 kcal/mol in both spin states,[24] and the energy required for the free radical is a little lower than the barrier for the rebound step. This result may suggest that the free radical can be generated before going down the potential energy surface to the product complex via TS2. An interesting point in the rebound process is the possibility of inversion of stereochemistry. Experimental evidence for that was obtained by Groves and co-workers,[4] Sligar and co-workers,[5] and White and co-workers[6] in various hydroxylation reactions mediated by P450. We think that the configurational inversion of substrate can occur in trajectory calculations if the reacting system has sufficient kinetic energy.

Dynamics of the H-Atom Abstraction. We carried out trajectory calculations of ethane hydroxylation mediated by a Compound I model of P450 on the doublet and quartet potential energy surfaces. The nuclei were propagated from a transition state in a reactant or product direction according to classical dynamics on a Born−Oppenheimer potential energy surface without taking quantum effects such as zero point energy or tunneling into account. Information from single trajectory calculations is of course limited, but they are useful for increasing our knowledge of the correct reaction pathway and the dynamic aspect in this very important enzymatic reaction. Although it is difficult at present to perform a statistical treatment, due to limited computational power, we hope to be able to calculate various thermodynamical properties from a large number of trajectory runs in the near future.

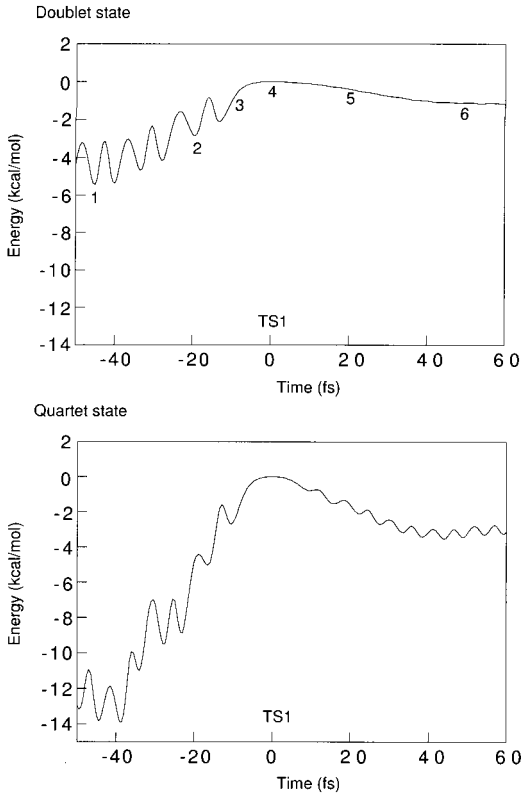

Figure 2. Energy profiles of the trajectory runs for the H-atom abstraction from ethane by a Compound I model.

Figure 2 shows computed potential energy profiles for the H-atom abstraction from ethane via TS1, the transition state for this chemical step. Here we defined the transition state as 0 fs in the time scale. First of all, we are able to confirm from these trajectory calculations that TS1 correctly connects the reactant complex and the intermediate complex; it is a true transition state for the H-atom abstraction. The kinetic isotope effects for the H-atom abstraction were calculated and analyzed in a previous study, the k_H/k_D values for CH_2DCH_3, CD_3CH_3, and C_2D_6 being 7, 11, and 13, respectively,[36] at 300 K from transition state theory. This result clearly demonstrates that not only the C−H(D) bond being cleaved but also other molecular moieties have significant effects on the kinetic isotope effect values. The k_H/k_D values become about one and half times larger in the temperature range 200−500 K if we take quantum tunneling effects into account according to Wigner's correction.[61] Since the mass of the hydrogen atom is small, quantum mechanical effects should play an important role in this chemical step.

Calculated snapshots about the H-atom abstraction step are displayed in Figure 3. The mechanistic picture obtained from

(58) Shaik, S.; Danovich, D.; Fiedler, A.; Schröder, D.; Schwarz, H. *Helv. Chim. Acta* **1995**, *78*, 1393.

(59) Schröder, D.; Shaik, S.; Schwarz, H. *Acc. Chem. Res.* **2000**, *33*, 139.

(60) Plattner, D. A. *Angew. Chem., Int. Ed. Engl.* **1999**, *38*, 82.

(61) Wigner, E. *J. Chem. Phys.* **1937**, *5*, 720.

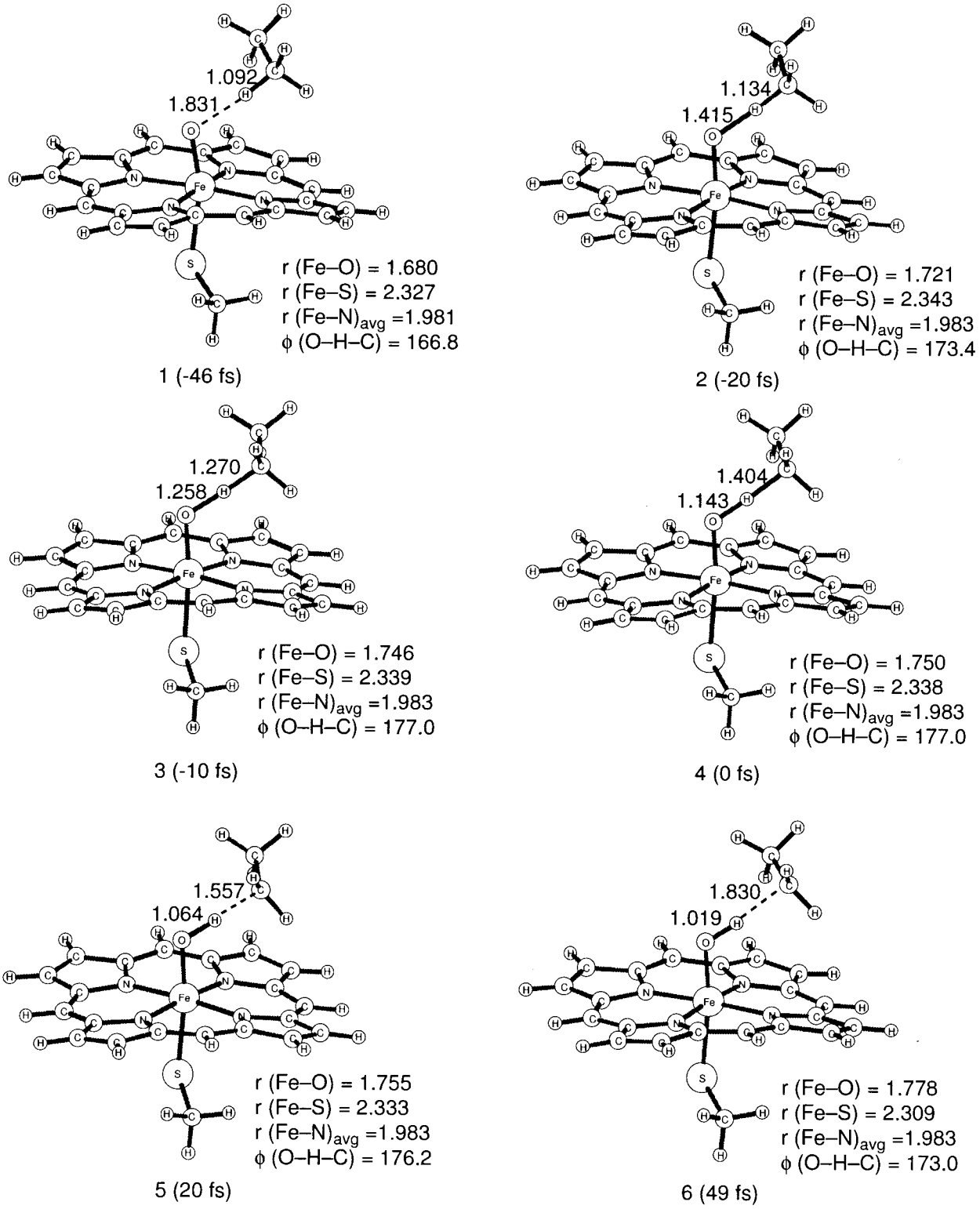

Figure 3. Structural changes in the trajectory runs for the H-atom abstraction from ethane in the doublet state.

the trajectory calculations is fully consistent with what we expect from the general features of the first half of the oxygen rebound mechanism. The principal reaction coordinate that can represent this chemical step is the C−H distance or the O−H distance while other geometrical parameters remain almost unchanged. The transition state is predicted to have the C−H distance of 1.404 Å (1.359 Å) and the O−H distance of 1.143 Å (1.183 Å) in the doublet state (in the quartet state). In the course of the reaction, the O−H−C bond is kept collinear and there is no direct interaction between the iron active center and the carbon atom. This structure is reasonable for the transition state of H-atom abstraction by Compound I of P450 because the iron active center is coordinatively saturated. The geometric features in this model enzymatic reaction are essentially identical with those in the direct H-atom abstraction from methane by the bare FeO^+ complex[56] and by diiron model complexes[62−66] that mimic the active species of soluble methane monooxygenase.

(62) Siegbahn, P. E. M.; Crabtree, R. H. *J. Am. Chem. Soc.* **1997**, *119*, 3103.
(63) Siegbahn, P. E. M. *Inorg. Chem.* **1999**, *38*, 2880.

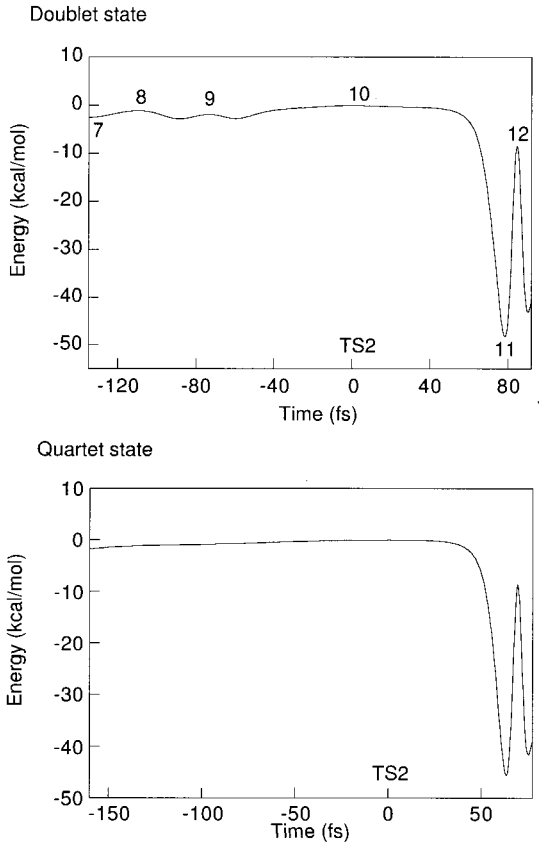

Figure 4. Energy profiles of the trajectory runs for the rebound process.

Dynamics of the Rebound Step. In the second half of the oxygen rebound mechanism, the iron−hydroxo complex and the ethyl radical intermediate are bound to form the product complex that involves ethanol as a ligand. This chemical step is highly exothermic and should proceed at no cost of energy, as shown in Figure 1, the driving force for this process being the great energetic stability of the product complex. We carried out trajectory calculations for the rebound step by supplying a small amount of kinetic energy to the transition state toward the forward or backward direction. Figure 4 demonstrates computed potential energy profiles for the rebound step of the iron−hydroxo complex and the ethyl radical intermediate via TS2, the transition state for this process. We also defined the transition state as 0 fs in the time scale. The reaction begins with the iron−hydroxo complex and the ethyl radical intermediate and ends with the formation of the product complex, the essential process in this reaction being the formation of the C−O bond. Since the reacting system passes over the transition state with a small velocity, the profile of the resultant potential energy is flat in the vicinity of the transition state. There is a jump in potential energy at 91 fs after the C−O bond formation is completed. This intriguing phenomenon arises from interconversion between the kinetic energy that the reacting system gains during the downhill process and the compressive energy of the C−O bond newly formed. A very similar phenomenon is observed in the methane to methanol conversion mediated by the bare FeO^+ complex.[37] The C−O distance gradually decreases as the reaction proceeds while the Fe−S, Fe−O, and

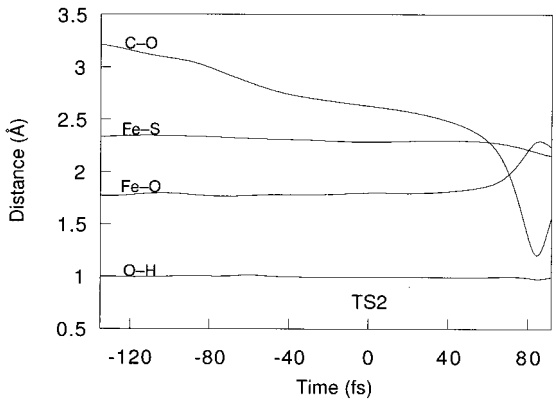

Figure 5. Changes in bond distances in the trajectory runs for the rebound process in the doublet state.

O−H distances remain almost constant, except in the final stages of the reaction, as shown in Figure 5. We see a sharp decrease in the C−O distance and a less significant increase in the Fe−O distance in the final stages of the trajectory run. The potential energy jump we see in Figure 4 occurs at this time. At the same time the Fe−S distance slightly decreases; thus, the Fe−O bond and the Fe−S bond work together in the hydroxylation reaction.

Calculated snapshots in the rebound process are displayed in Figure 6. We can see small structural changes in the Fe−OH moiety and the C−O distance. Although the final structure in the doublet state dynamics in Figure 4 is not reported here, its structure is closer to the structure of snapshot **11** than to that of **12**. The H−O−Fe−C dihedral angle corresponds to the principal reaction coordinate for this process; this quantity goes up from 18° to 40° in the initial stage, goes down to nearly 0° at −74 fs, and again goes up to 90° in the transition state, as shown in Figure 7. Of course, this dynamical feature will be significantly changed if the trajectory calculation is started under different initial conditions. When sufficient kinetic energy is supplied to this rotational mode, this rebound process should efficiently take place, leading to the product complex.

Although our trajectory calculations suggest that 200 fs is likely to be a typical value for the time required for the rebound process, we cannot jump to the conclusion that this result has direct relevance to short radical lifetimes (τ = 80−200 fs) estimated from recent radical-clock experiments. We can say that 200 fs is a value obtained under specific initial conditions, in which a small amount of kinetic energy (0.1 kcal/mol) is supplied to the transition state exactly along the reaction coordinate. Clearly, a huge number of trajectory calculations started under various initial conditions and statistical treatment are necessary for further quantitative arguments. Recent advances in computer technology will allow us to perform such high-level statistical treatment from a number of trajectory runs within a few years.

Energy Distribution to Vibrational Modes. We can learn from trajectory calculations what vibrational modes are activated in the hydroxylation reaction. Figure 8 shows changes in the amplitudes of normal coordinates along the reaction pathway to the H-atom abstraction via TS1 in the low-spin doublet state. A large part of the energy is distributed to the C−H and O−H stretching modes before and after the transition state, respectively, and its remaining small part is distributed to the Fe−O and Fe−S stretching modes. It is more interesting to look at whether the kinetic energy is distributed to the well-known marker bands of the porphyrin ring.[67,68] Information from the trajectory calculations can tell us how the extra kinetic energy

(64) Basch, H.; Mogi, K.; Musaev, D. G.; Morokuma, K. *J. Am. Chem. Soc.* **1999**, *121*, 7249.
(65) Yoshizawa, K.; Suzuki, A.; Shiota, Y.; Yamabe, Y. *Bull. Chem. Soc. Jpn.* **2000**, *73*, 815.
(66) Gherman, B. F.; Dunietz, B. D.; Whittington, D. A.; Lippard, S. J.; Friesner, R. A. *J. Am. Chem. Soc.* **2001**, *123*, 3836.

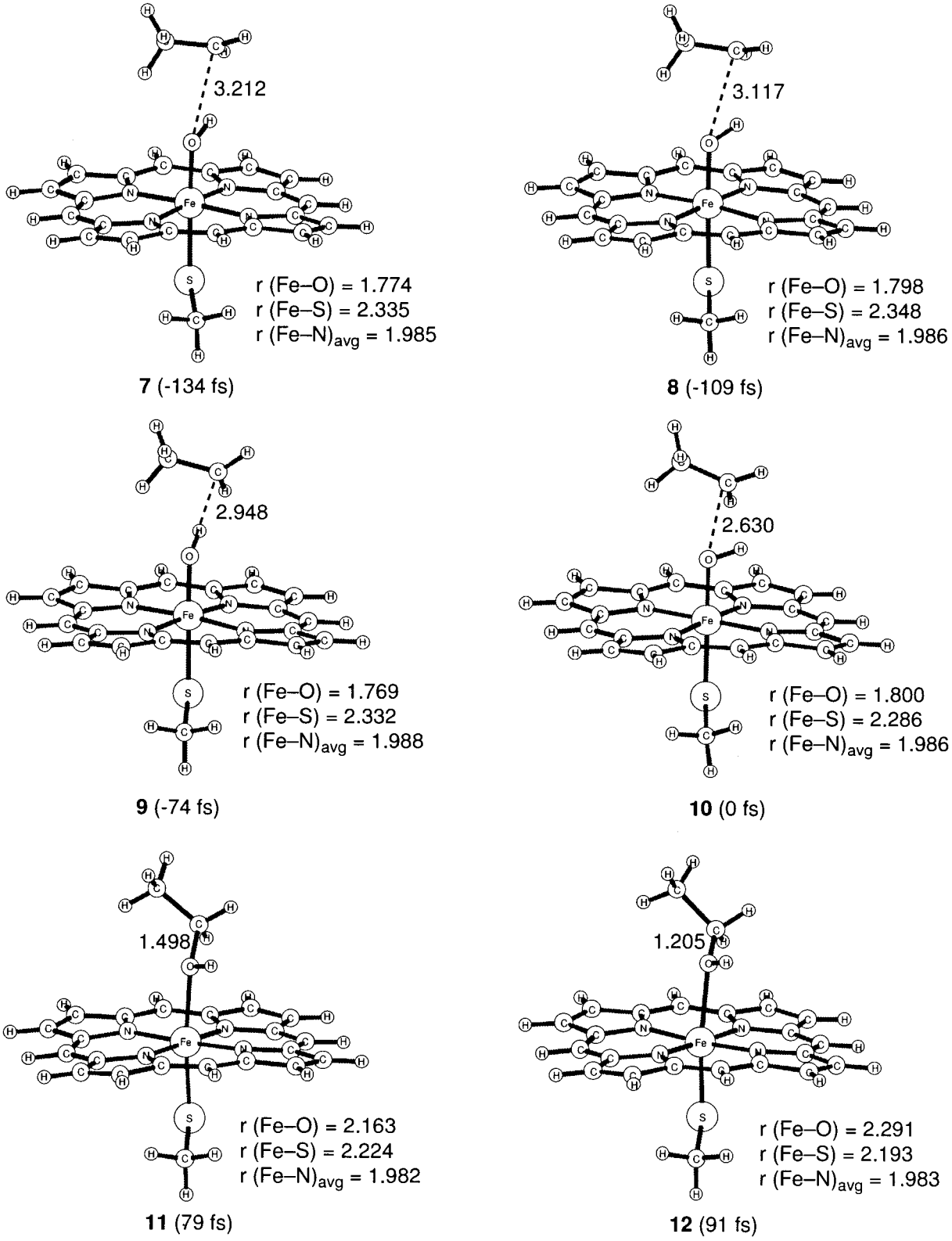

Figure 6. Structural changes in the trajectory runs for the rebound process in the doublet state.

is transferred to the surrounding residues of the active site through the porphyrin ring. Figure 8 demonstrates that the ν_3 mode is highly excited during the reaction and that the ν_4 mode is also excited before TS1. Since the ν_3 and ν_4 modes explicitly involve Fe−N stretching motion, as indicated in Chart 1, these vibrational modes of the porphyrin ring should play an important role in the energy transfer during the hydroxylation reaction.

Figure 9 presents changes in the amplitudes of normal coordinates along the reaction pathway of the rebound process

(67) Li, X.-Y.; Czernuszewicz, R. S.; Kincaid, J. R.; Su, O.; Spiro, T. G. *J. Phys. Chem.* **1990**, *94*, 31.

(68) Li, X.-Y.; Czernuszewicz, R. S.; Kincaid, J. R.; Stein, P.; Spiro, T. G. *J. Phys. Chem.* **1990**, *94*, 47.

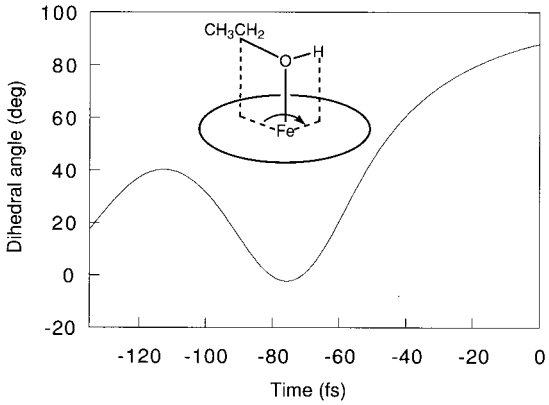

Figure 7. A change in the H−O−Fe−C dihedral angle in the rebound process in the doublet state.

via TS2 in the low-spin doublet state. In this process the iron−hydroxo complex and the ethyl radical intermediate come into contact to form a C−O bond that leads to the ethanol complex. The amplitude of each normal coordinate is small in the vicinity of the transition state at $t = 0$ because the reacting system has no kinetic energy there. After TS2, most of the kinetic energy is distributed to the stretching mode of the C−O bond that is newly formed in the rebound process, thus the amplitude of this stretching mode is significant. The porphyrin marker modes of ν_3 and ν_4 that involve explicit Fe−N stretching motion are also enhanced in the rebound process.

Concluding Remarks

We investigated dynamic aspects of alkane hydroxylation mediated by Compound I of cytochrome P450 from classical trajectory calculations at the B3LYP level of density functional theory. We propagated the nuclei of the reacting system from a transition state to a reactant or product direction on a Born−Oppenheimer potential energy surface according to classical dynamics with the velocity Verlet algorithm. Geometric and energetic changes in both low-spin doublet and high-spin quartet states are followed along the ethane to ethanol reaction pathway, which is partitioned into two chemical steps: the first is the H-atom abstraction from ethane by the iron−oxo active species of Compound I and the second is the rebound step in which the resultant iron−hydroxo complex and the ethyl radical intermediate come into contact to lead to the ethanol complex. In the H-atom abstraction, molecular vibrations of the C−H bond being dissociated and the O−H bond being formed are significantly activated before and after the first transition state, respectively. The principal reaction coordinate that can represent the first chemical step is the C−H distance or the O−H distance while other geometric parameters remain almost unchanged. The rebound process begins with the iron−hydroxo complex and the ethyl radical intermediate and this process ends with the formation of the ethanol complex, the essential process in this reaction being the formation of the C−O bond. The H−O−Fe−C dihedral angle corresponds to the principal reaction coordinate for the rebound step. When sufficient kinetic energy is supplied to this rotational mode, the rebound process should efficiently take place to form the ethanol complex. Classical trajectory calculations suggested that about 200 fs is required for the rebound process under specific initial conditions, in which a small amount of kinetic energy (0.1 kcal/mol) is supplied exactly to the second transition state along the reaction coordinate. We finally investigated an important issue regarding what normal modes of vibration are activated during the hydroxylation reaction in detail from trajectory calculations. A large part of the kinetic energy is distributed to the C−H and O−H stretching modes before and after the transition state for the H-atom abstraction, respectively, and the remaining small part of the kinetic energy is distributed to the Fe−O and Fe−S stretching modes and some characteristic modes of the porphyrin

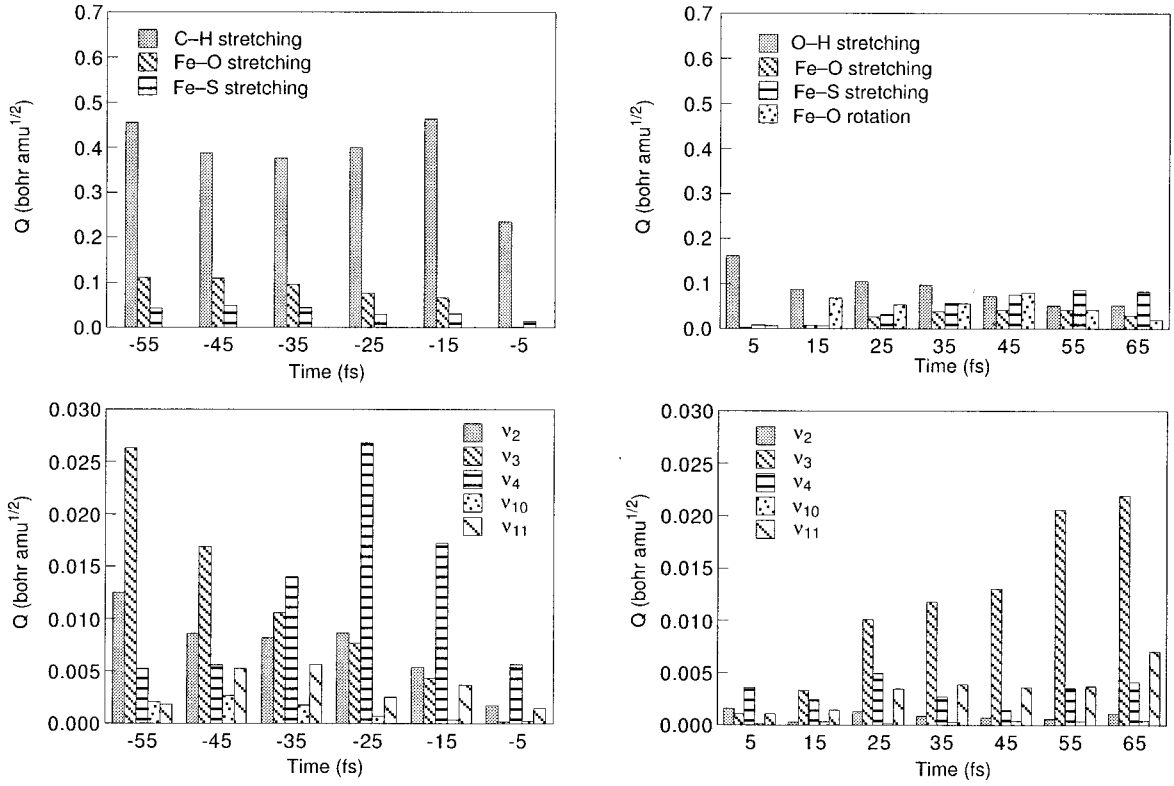

Figure 8. Changes in the amplitudes of normal coordinates in the trajectory runs for the H-atom abstraction from ethane in the doublet state.

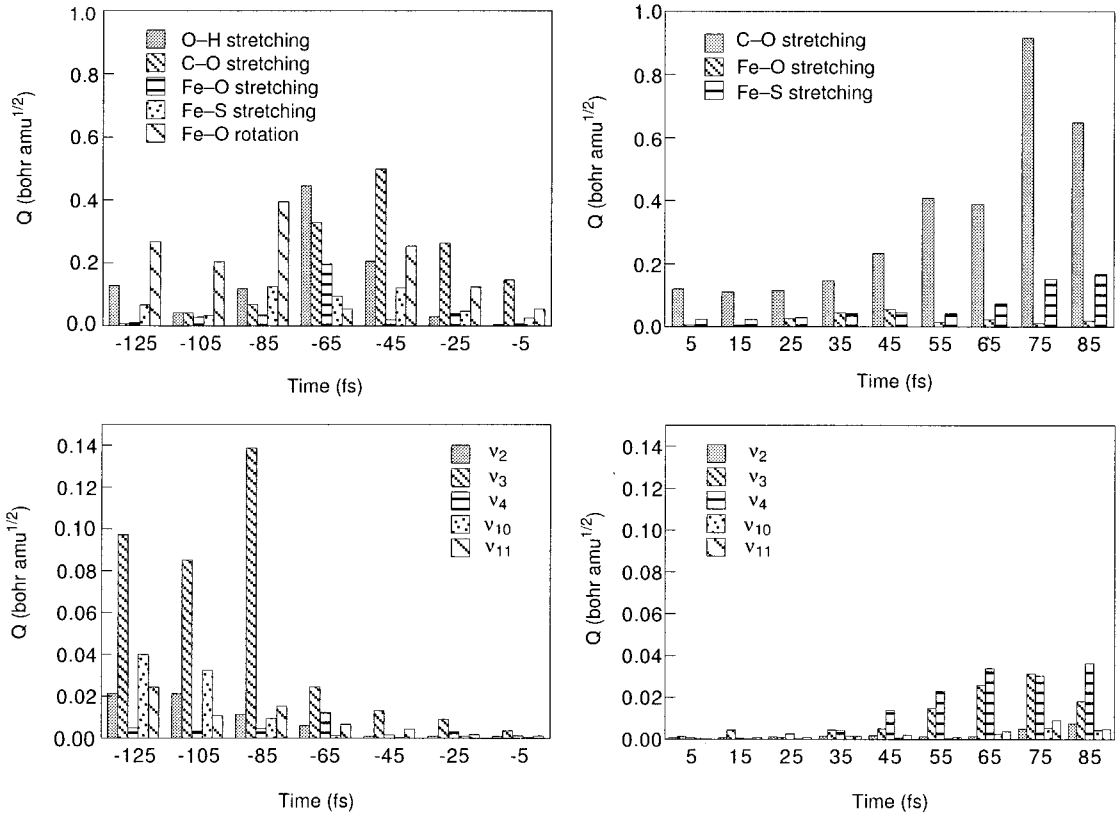

Figure 9. Changes in the amplitudes of normal coordinates in the trajectory runs for the rebound process in the doublet state.

Chart 1

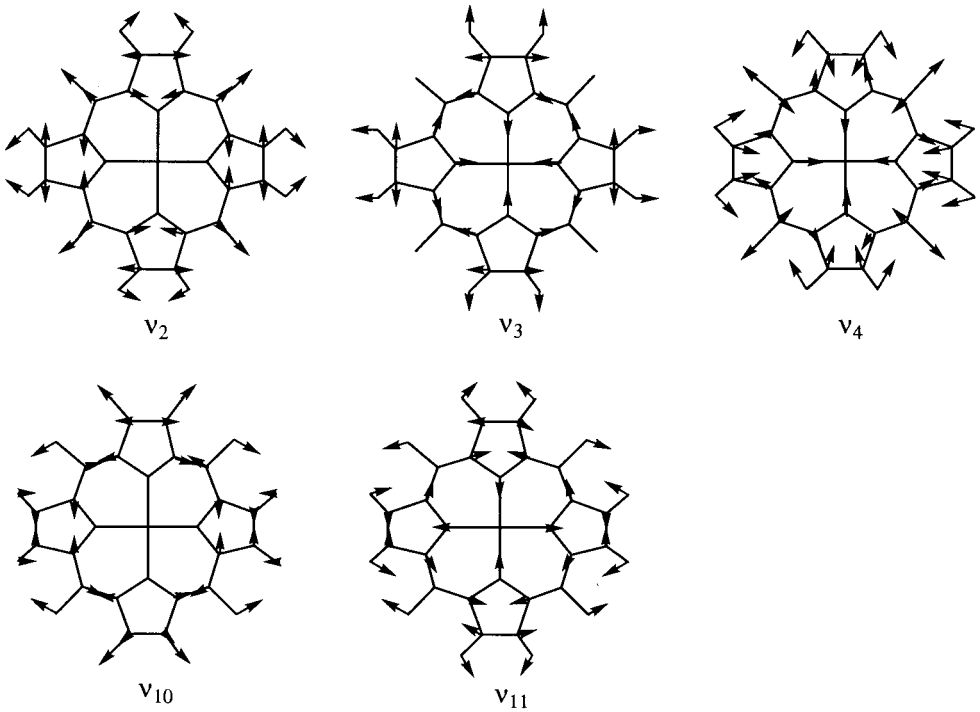

ring. The porphyrin marker modes of ν_3 and ν_4 that involve Fe−N stretching motion are enhanced in the course of the hydroxylation reaction mediated by Compound I of cytochrome P450. These vibrational modes of the porphyrin ring would play an important role in the energy transfer during the hydroxylation reaction.

Acknowledgment. K.Y. acknowledges a Grant-in-Aid for Scientific Research on the Priority Area "Molecular Physical Chemistry" from the Ministry of Education, Culture, Sports, Science and Technology of Japan and the Iwatani Naoji Foundation's Research Grant for their support of this work. Computations were partly carried out at the Supercomputer

Laboratory of Kyoto University and at the Computer Center of the Institute for Molecular Science.

Supporting Information Available: Three figures of changes in bond distances in the trajectory runs for the rebound process in the quartet state, structural changes in the trajectory runs for the rebound process in the quartet state, and a change in the H−O−Fe−C dihedral angle in the rebound process in the quartet state (PDF). This material is available free of charge via the Internet at http://pubs.acs.org.

JA010593T